Structure and Properties of Hybrid Coatings

A.D. Pogrebnjak*, Yu.A. Kravchenko*,V.V. Vasilyuk*, Yu.N. Tyurin**, D.L. Alontseva***, Sh.M. Ruzimov****, V.V. Ponaryadov***

** Sumy Institute for Surface Modification, P.O.Box 163, St.Romenskaya 87, Bld.”M”, 40030 Sumy, Ukraine; e-mail: apogrebnjak @simp.sumy.ua*
*** O.E. Paton Electric Welding Institute, NAS of Ukraine, Kiev, Ukraine*
**** Belarus State University, Minsk, Belarus*
***** National University of Uzbekistan, Tashkent, Uzbekistan*

Abstract – This review report presents both the results obtained by the authors and those of other authors concerning investigations of structure and properties of hybrid coatings. Examples of such coatings as Al_2O_3/Cr/TiN/steel, NiCr/steel; CrNiBSi/steel and others before and after electron beam irradiation had been considered. In these coatings the thickest layer was deposited using the high velocity pulsed plasma jet, all others being deposited in vacuum by the vacuum arc source or implanter. Advantages of the high velocity pulsed plasma jet in comparison with other technologies had been demonstrated. A wide spectrum of analyzing methods had been applied for analyses: TEM, SEM with EDS, RBS, NRA, SIMS, XRD, tests for corrosion, wear, adhesion and hardness.

1. Introduction

Today the protecting coatings deposited to tools applied for electro chemical and chemical equipment attract high interest. It is known, that such ways of treatment as the ion implantation, ion assisted deposition of thin films, electron beam treatment, coating deposition using high velocity plasma jets, etc. [1–4] cannot directly lead to the desired effect. Therefore recently to solve some applied problems one has to apply the combined methods of treatment, which allow us to resolve serious problems in material science (aviation, space, automobile industry, shipbuilding, etc). On the other hand, it is known, that such tools as the blades of acid pumps need high degree of adhesion of a coating to a tool substrate surface, low porosity and presence of passivating elements as Cr, Ti, etc.

In such a way, the goal of this work was to study the structure and element composition of the combined coating on Al_2O_3/Cr/TiN base, which was deposited to the substrate of steel 3 (0.3 wt.%C) before and after electron beam irradiation, as well as to study the servicing characteristics of the resulting hybrid coating. A special attention had been paid to the processes of diffusion and mass transfer.

The protecting hybrid coatings had been deposited on thin samples (0.3 mm thickness) of an austenite stainless steel 321 (18%Cr, 9%Ni, l%Ti, Fe the rest) in the following way. Using a high velocity pulsed plasma Jet of the apparatus “IMPULSE 5” [5–7], we had deposited a basic coating of aluminum oxide of 45 to 65 μm thickness. Al_2O_3 α powder of 27 to 56 μm grain dimension served as an initial one. A detonation frequency (a number of pulses) was 4 Hz. Energy expenditures for every plasma pulse was 2.5 to $3.5 \cdot 10^3$ J. A distance to the substrate was 40 cm, a spot diameter was 33 cm. To improve the coating corrosion characteristics in a sulphuric acid solution, a titanium nitride (TIN) trace of 1.2 to 2 μ thickness was deposited to Al_2O_3 coating using a vacuum arc source of “Bulat 5M” type. To improve the adhesion, Cr sublayer of 0.2 to 0.5 μm thickness was deposited prior to TIN layer.

Further, the surface of the hybrid coating was irradiated by a high current electron beam (HCEB) of' “U 212” apparatus manufactured at the O.E.Paton Electric Welding Institute, Kiev, Ukraine. The beam energy density was chosen in that way that the coating Al_2O_3/Cr/TiN coating was totally melted but the substrate was melted partially. The accelerating voltage was 30 kV, the beam current was 35 and 20 mA, the amplitude reached 15 mm, the scanning rate was 2 to 30 m per hour for series 2 and 15 m per hour for series 3. The features of HCEB treatment this time consisted in that the diameter of the electron beam was 3 mm for a scanning step 0.9 mm. This allowed us to form a strip like micro structure in the surface the strips with a melted coating alternated with non melted ones. Three series of sampled had been used: Series 1 was an initial coating Al_2O_3/Cr/TiN non irradiated; Series 2 was subjected to HCEB irradiation with partial melting of the coating (20 mA current density); Series 3 was subjected to HCEB irradiation with total melting of the coating and partial melting of the substrate.

We had performed also mechanical tests for hardness, adhesion and corrosion resistance in the sulphuric acid under 200 to 400 °C. To analyze the element composition we applied the proton back scattering of “SOKOL” accelerator INTs KhFTI with the starting energy 1.55 MeV. Studies of Auger spectrometry had been performed using the Scanning Auger Multi probe apparatus PHI 660 (Perkin Elmer, USA). The element distribution over depth was studied by ion sputtering of the hybrid coating layers. Ar ions of 3.5 keV energy were applied for sputtering. The surface was studies using the scanning electron microscope REMMA 102 (Selmi, Sumy, Ukraine) with micro analysis EDX. The phase composition (XRD) was studied using the apparatus “DRON 2” (St.Peterburg, Russia) in $Cu_{\alpha}K_{\alpha}$ emission.

2. Experimental Methods

In our experiments we applied SEM (REMMA 102 with EDX, Selmi, Sumy, Ukraine), XRD analysis (DRON 2, St.Peterburg, Russia), AES (the Scanning Auger Multi probe, PHI 660, Perkm Elmer (USA).

The micro hardness was measured using PMT 3 apparatus with a diamond Vickers pyramid with the indenter loads of 20, 50 and 100 g over the surface and the transversal and angular cross sections.

The wear resistance was tested using the apparatus CMTC 2 (Ukraine) according to the scheme a plane cylinder in a medium of technical petrolatium (Vaseline). Corrosion resistance of the modified and initial surfaces was tested using the electro chemical equipment (Bank Wenking Potentio Galvanostat PGS 81R) and a cell Princeton Applied Research corrosion test. A solution of 0.5 M H_2S0_4.

A material for production of a corrosion resistant coating with high servicing characteristics served a powder PGAN 33. Its composition was: Ni the base; Cr 22 to 24 wt.%; Mo about 4 wt.%; Si about 2 wt.%; W l to 1.5 wt.%, B about 2 wt%. One should note that such additions as Si and B were introduced in the powder composition with the purpose to decrease the forces of surface tension in the melted coating during the period of its modification by the concentrated energy flows. Mo and W played the role of doping elements, which allowed us to increase the hardness pf the produced coatings. The powder Coating of the nickel alloy (60 to 110 μm thickness) had been deposited to the low carbon steel 3 (St 3) substrate using the apparatus “IMPULSE 5”. The operation regimes were the following: the capacitor bank capacity was 800 μΦ, the frequency of pulse repetition was 5 Hz, the plasma jet velocity reached 7.5 to 7.8 km/sec, the plasma jet temperature was $3 \cdot 10^4$.

Expenditures of the combustion mixture components reached 2 m^3 per hour. We applied the eroding Mo electrode. The distance, from which the coating was deposited, was about 40 mm.

Subsequently, a part of the samples with deposited coatings was melted by the electron beam using the apparatus U 212. We had chosen two regimes of the electron beam treatment:

1. till total melting of the coating and the top substrate layer to ≤ 40 μm;

2. till total melting of the coating and partial melting of the substrate to 150–200 μm depth.

The electron beam velocity in both cases was 80 m per hour, and the width of the treated path was about 12 mm.

3. Experimental Results and Discussion

Figure 1 show the image of the hybrid coating Al_2O_3/Cr/TiN surface morphology before and after HCEB irradiation. One can see a high surface roughness [8], which is typical for the coatings produced by the plasma detonation way of treatment, since the deposited in vacuum films of Cr and TIN copy the coating surface relief (Fig. l).

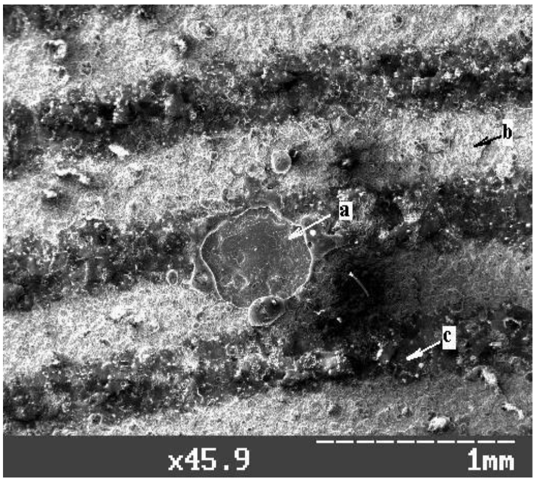

Fig. 1. Surface structure of the hybrid coating Al_2O_3/Cr/TiN, which had been treated in a combined

HCEB irradiation resulted in formation of the stripe like surface structure. One can observe alternation of light and dark strips. Points in these trips mark those places, at which we had performed micro analysis. We should also note that a formation of a melted droplet (TIN and Cr deposition) had been performed without segregation, therefore the “droplet” fraction, which was seen in the hybrid coating surface, was formed. The dark strips indicate the initial surface (non irradiated by HCEB), the light ones indicate the HCEB irradiated regions. Micro analysis had been performed using the X ray spectrometer with a WDS 2 attachment, manufactured on the basis of a semiconducting Si (Li) detector.

Figure 2 shows the spectra taken in various surface regions. The spectra taken in round inclusions (the droplet fraction) indicate the following elements: Ti, Cr, Fe (see Fig. 2a, b, c). A dominating element is titanium.

Also we had found that the concentration of these elements in the above region (the melted droplet) was not constant at various points. In addition, we had found presence of Al.

The regions, which were not subjected to HCEB irradiation contain: 13.9 wt.% of Al; 48.2 wt.% of Ti; 0.03 wt.% of Cr; 0.42 wt.% of Fe. As for the melted regions, they contain: about 55 wt.% of Al; 0.5 wt.% of Ti; 0.2 wt.% of Cr and 0.8 wt.% of Fe.

In details, the element composition of the hybrid coating had been studied using BS method for two different conditions.

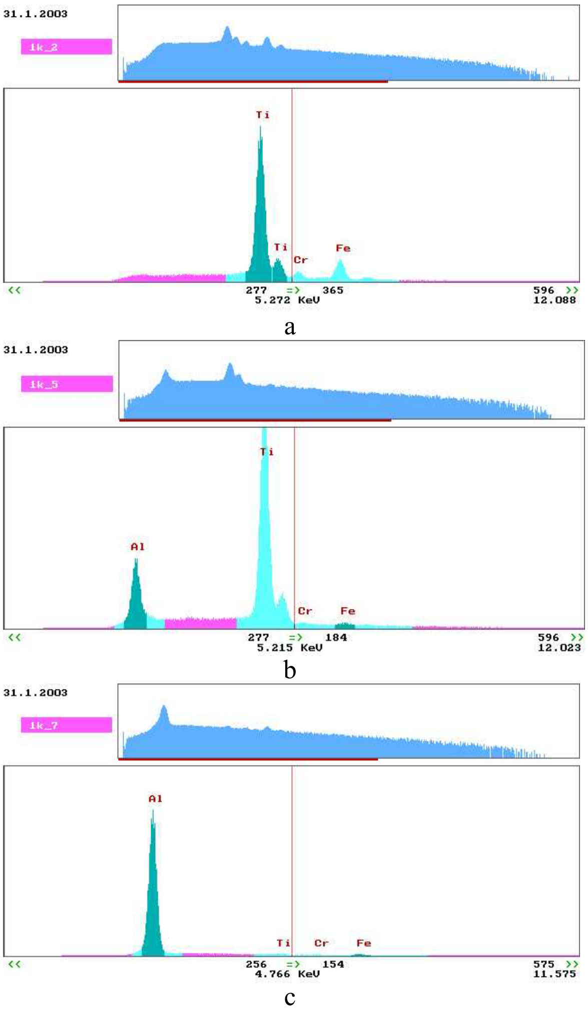

Fig. 2. Element analysis spectra of the hybrid coating composition taken at the following points: a – the region of "drop fraction" at the bottom of the surface crater; b – the light region; c – the dark region

Figure 3 shows the energy spectra of protons with the initial energy of 1.55 MeV, back scattered from non irradiated and HCEB melted samples (low and high HCEB density).

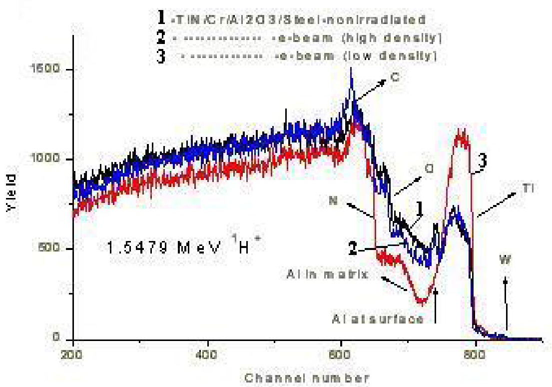

Fig. 3. Energy spectra of proton back scattering with the initial energy 1.55 MeV from the non treated and HCEB melted samples (at low and high HCEB energy density): series 2 and series 3

Data handling of the spectra had demonstrated the presence of aluminum, titanium, oxygen, and nitrogen in the near surface layers of the coatings of melted samples. BS analysis also indicated an increase in oxygen concentration in the melted samples.

In the near surface layers of non irradiated samples, the oxygen concentration was essentially lower. According to obtained results, after electron beam annealing (melting), in the coatings we observed a decrease in the titanium atomic content and a simultaneous broadening of the distribution profiles into the coating depth.

Figure 4 shows the efficient Ti concentration depth profiles in the hybrid coating Al_2O_3/Cr/TiN.

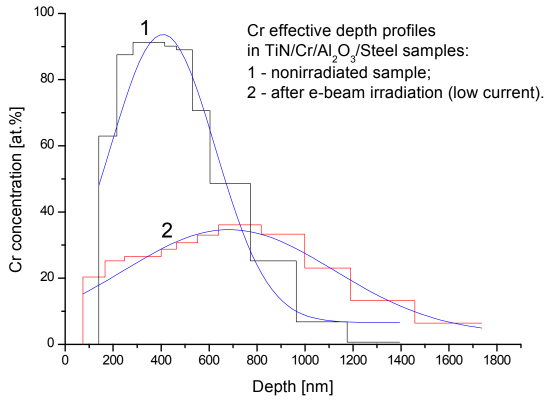

Fig. 4. The efficient Ti concentration depth profiles in the hybrid coating Al_2O_3/Cr/TiN (the profiles had been extracted from the proton BS spectra using DVBS code)

The profiles were extracted from the proton BS spectra using the DVBS code. Then the depth profiles were fitted by Gaussian curves. The Figure shows that the histograms of Ti concentration distribution are good fitted by the curves. In its turn, fitting allowed us to obtain the parameters of normal distribution, which were used to estimate Ti effective diffusion coefficient for electron beam annealed samples. It had been found to be equal to $D_{effTi} = 2.4 \cdot 10^8$ cm^2/s. The linear fitting of Ti effective diffusion coefficient in Arrhenius coordinates in the ion implanted $A1_2O_3$ obtained in [9] was extrapolated to the value region of about $2.4 \cdot 10^{8}$ cm^2/s.

An annealing temperature $T = 1170$ °C was found corresponding to the above mentioned value of the diffusion coefficient.

The same samples had been studied for the phase composition (XRD analysis) of the hybrid coatings Al_2O_3/Cr/TiN. The results show that a basic matrix element is γ Fe (fee) with the lattice parameter 3.592Å. The XRD analysis allowing for an integral characteristic for the layer of several micro meters shows that the hybrid coating is a many phase compound. In addition to the basic powder α Al_2O_3, we observed γ Al_2O_3, β $A1_2O_3$, TIN, and Cr. We had evaluated a percentage ratio of the phases in the coatings after double treatment regimes (series 2, series 3).

The presented calculations allowed us to conclude about strong influence of the surface modification by HCEB on the lattice parameters of the coating composition elements.

We also had found the changes in $A1_2O_3$ lattice parameters, which seemed to be related to the formation of residual compressing stresses (*series 1* not subjected to HCEB treatment: a = 4.773 Å, c = 13.581 Å, c/a = 2.87 Å; *series 2* HCEB treated: a = 4.773 Å, c = 12.996 Å, a/c = 2.72 Å; *series 3:* a = 4.76 Å, c = 12.878 Å, c/a = 2.71 Å).

In the initial state, before HCEB treatment the lattice parameter of titanium nitride was equal to 4.264 Å, and after HCEB irradiation under partial melting it was 4.221 Å. After HCEB irradiation till total meting of the combined coating the lattice parameter was 4.247 Å. We had found also the changes in Cr lattice parameter (series 1 a = 2.879 Å; series 2 and 3 a = 2.868 Å).

The additional analysis had been performed using Auger electron spectrometry for better interpretation of the results of element analysis.

Figure 5 shows the concentration profiles of the coating elements vs the depth of the hybrid coating. The approximated evaluation of the depth demonstrated that after Ar ion sputtering for 30 min, the layer thickness was 2.5 to 3 µm. One should note that we found a wide spectrum of elements and their composites (compounds or clusters) in the coating. Near the surface, we found high Ti and N concentration, followed by Cr and Al peaks, when the etching time was increased, as well as Cr_2, Cr_3Fe_3 clusters.

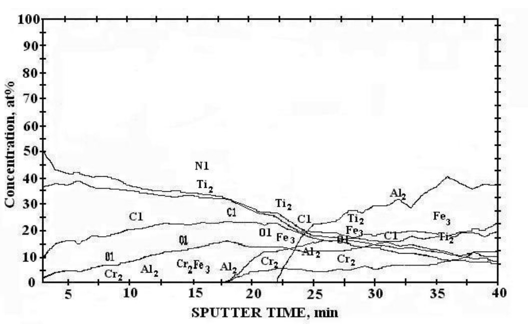

Fig. 5. Depth distribution of AES spectra for sputtered Al_2O_3/Cr/TiN hybrid coating (sputtering had been performed using Ar^+ ion beam with about 5 keV energy)

A decrease in the corrosion potential E as well as a decrease in the corrosion currents τ_{corr} and the passivation τ_{pas} in the case of the electron treatment of Al_2O_3/Cr/TiN coating demonstrate good corrosion resistance of the hybrid coating in the sulphuric acid.

We may assume that this increase in the corrosion resistance is related to the decrease in the amount of perforating pores in $A1_2O_3$, the increase in the coating thickness due to TiN and Cr, as well as its mixing with the ceramic layer.

One should also note that the coating density in $A1_2O_3$ initial state is 3.9 g/cm^3. At the same time, from literature it is known that α Al_2O_3 has 3.9 g/cm^3 density, and the coating adhesion to the substrate (without HCEB treatment) is 40 to 65 MPa. However, HCEB irradiation in the case of series 3 resulted in the adhesion increase up to 140–160 MPa (which seemed to be related also to the melting and liquid phase mixing).

The coating hardness without HCEB irradiation was $1.3 \cdot 10^4$ N/mm^2. After HCEB irradiation (series 2) it was about $1.6 \cdot 10^4$ N/mm^2, $1.78 \cdot 10^4 \pm 0.8$ N/mm^2. In such a way, after HCEB irradiation the hardness increase became evident.

Figure 6 shows the XRD profiles taken from the coating surface layer melted by the electron beam.

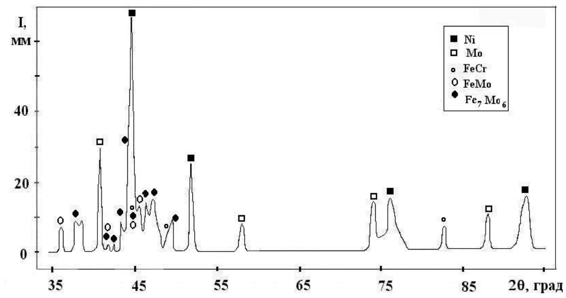

Fig. 6. A fragment of the diffraction pattern obtained from the surface of PGAN 33 powder coating

According to the performed calculations, such elements as Ni (48 wt.%) and Mo (20 wt.%) are the basis of the coating. Evaluation of Ni lattice parameters demonstrated that Ni lattice underwent some changes. Appearing tensing stresses increase the lattice parameter: a (Ni) = 3.53 Å (a_{table}(Ni) = 3.524 Å) [10]. The melting initial powder (in the coating) formed a compound FeCr, which mass fraction was about 15%. We had found also the inter metalloid compound Fe_7Mo_6, and when the background level was increased to 2θ ~ (42–50)°, we had revealed FeMo. The mass ratio of these inter metalloids was 12 wt.% and 4 wt.% of the total composition of the coating surface layer [11].

Figures 7,a and 7,b show the hardness distribution over the sample depth after plasma detonation deposition without melting (a) and after total melting of the coating and partial meting of the surface substrate layer by the electron beam (b).

As it is seen from these Figures, a maximum value of micro hardness was found in the samples, which were treated by plasma detonation (or high velocity pulsed plasma jet). The coating thickness reached 170 µm, but the increased hardness was found almost till the depth of 300 µm. At the same time, the electron beam irradiation resulted in some decrease in the maximum hardness value from 750 ± 30 to 320 ± 30 kg/mm^2. However, the obtained dependences had two maxima: one of them was near the surface, another one was at the depth of about 300 µm. A total depth of the hardened layer reached about 500 µm, i.e. the hardened layer was two times thicker.

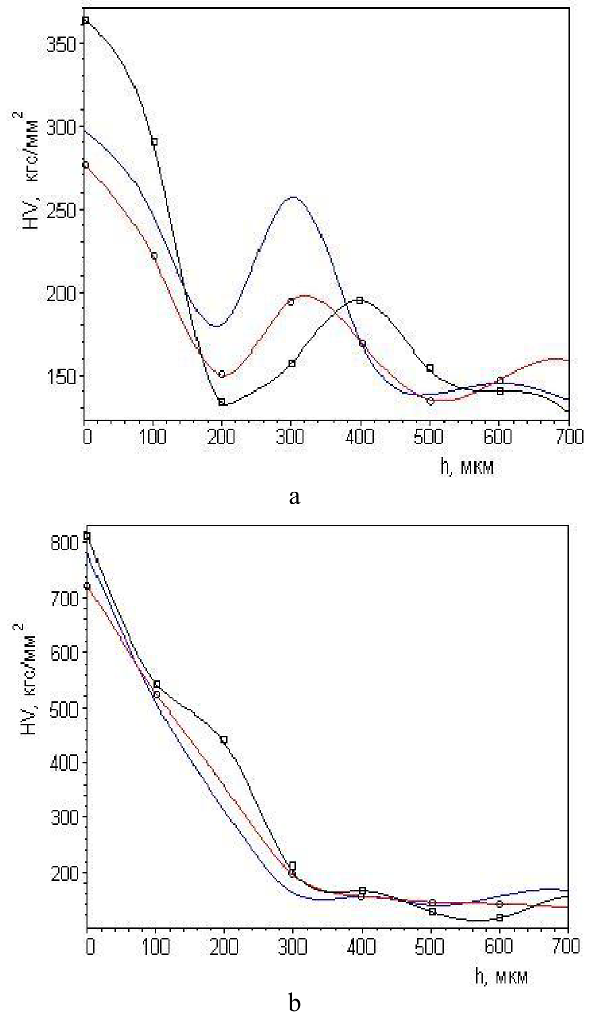

Fig. 7. Dependence of micro hardness on the depth of coating surface layer of Ni alloy (PGAN 33 was the base): a – after plasma detonation deposition and subsequent electron beam irradiation (melting); b – after coating deposition only

Figure 8 shows friction wear dependences for the coating surfaces treated by the plasma detonation with subsequent electron beam melting. As one can see in the Figure, the highest degree of wear was found in the initial material; in the coatings treated by plasma detonation without electron beam irradiation we found lower degree of wear; and the lowest one was found in the samples subjected to the subsequent electron beam melting (under lower energy density), i.e. a treated cylinder fretted for 25 min demonstrated difference in the wear, which was about 2.5 times lower than that for the initial one. The lowest wear was found in the samples, which were treated using a combination of regimes, as a result of which we managed to melt the coating and the substrate till the depth exceeding the coating thickness.

Therefore, we should like to underline that, in spite of the decrease in the coating micro hardness, which occurred after the electron beam treatment, the friction wear nevertheless remained significantly lower than that of the non treated samples.

It seems that it can be explained by phases with Mo basis, which were formed in the process of mixing, as well as by enrichment of the coating by iron, which diffused from the substrate. In addition, in the surface we found a definite oxide concentration (the results of element and micro analyses). The EDX micro analysis had demonstrated that, indeed, in the surface layer there were the regions with high Fe or Mo contents. We should note that Mo could penetrate as a result of evaporation (erosion) of the inside electrode, and Fe could came only from the substrate as a result of a convective metal motion occurring in a liquid phase.

Evaluations of the efficient diffusion coefficient in the substrate, which were derived from Ni concentration profile, demonstrated the value close to 10^5 cm/s.

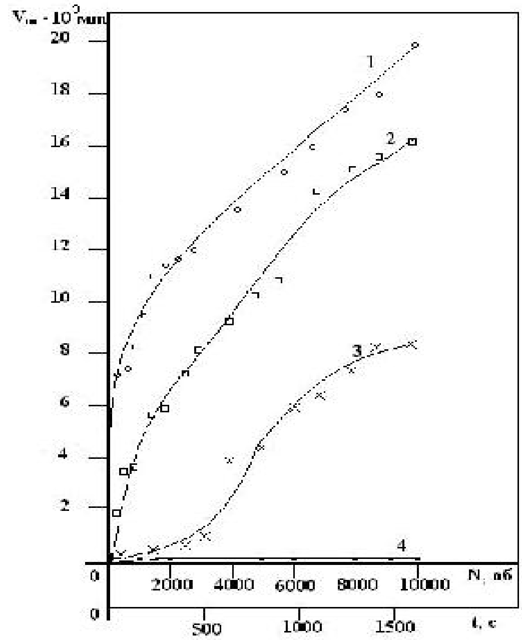

Fig. 8. Dependences of the dry friction wear for powder coatings on Ni base (PG 10N 01)

This corresponded to the liquid phase diffusion coefficient. However, they were essentially different for Fe and Mo, i.e. the mass transfer rate depended essentially on the element mass and initial distribution of impurity (before electron beam treatment).

4. Conclusions

Therefore, the deposition of the hybrid coatings of Al_2O_3/Cr/TiN and the subsequent HCEB treatment in two regimes (the third regime resulted in a total melting of the coating and a partial melting of the austenite stainless steel substrate) led to a change in the coating phase composition (XRD results), the element transfer, in particular, Ti (AES, BS and micro analysis results), as well as significant changes of the servicing characteristics, such as the adhesion, hardness, and the corrosion resistance in the sulphuric acid.

The performed studies of the element composition of powder coatings tiad demonstrated that the main component of the resulting coatings was Ni remaining even after electron beam treatment. The efficient coefficient of mass transfer, which was determined using Ni distribution in the substrate, was equal to $6 \cdot 10^5$ cm^2/s, which corresponded to the diffusion coefficient in the liquid phase.

We should underline different meanings of the coefficients for various metals, for example, Cr and Mo.

Electron beam irradiation induced the appearance of Fe in the coating. We had found I relation of the phase and chemical compositions and the surface morphology of the locating after the duplex treatment to the mechanical characteristics: the micro hardness, friction wear, corrosion resistance in acidic media and a sulphuric acid solution.

Appearing new phases, a decrease of grain dimensions from 10 s of micro meters to hundreds of nano meters, “healing” of the pores, the mass transfer, and possibly, a decrease of roughness seem to serve the basis for changing of servicing characteristics.

5. Acknowledgements

This work had been performed within the frame of the Project “Oxidation and Corrosion Behaviour of Pulsed Plasma Modified Metallic Alloys” supported by NATO Collaborative Linkage Grant No. PST 978157. The authors are grateful to Dr. V.S. Kshnyakin and M.V. Il'yashenko, and Prof. P. Misaelides for their interest in this study and help. This study had been also partly supported by the Ministry of Education and Science of Ukraine (Project No. M/0354 2003 and project No. 3078 STCU).

References

[1] A.D. Pogrebnjak, A.D. Mikhaliov, N.A. Pogrebnjak et al., Phisics Letters **A**. **241**, 357 (1998).

[2] A.D. Pogrebnjak, S. Bratushka, V.I. Boyko et al. NIM **B. 145**, 373 (1998).

[3] A.D. Pogrebnjak, A.G. Lebed’, Yu.F. Ivanov. Vacuum **63**, 483 (2001).

[4] V.I. Boyko, A.N. Valyaev, A.D. Pogrebnyak, Physics Uspekhi **42(II)**, 1139–1166 (1999).

[5] Yu.N. Tyurin and A.D. Pogrebnjak. Surf. and Coat. Tech. **111**, 269 (1999).

[6] A.D. Pogrebnjak, M.V. Il'yashenko, O.P. Kul’ment’eva, V.S. Kshnykin, A.P. Kobzev, Yu.N. Tyurin, O.P. Kolisnichenko, Vacuum **62**, 21 (2001).

[7] A.D. Pogrebnjak, Yu.N. Tyurin, Yu.F. Ivanov, A.P. Kobzev, O.P. Kul’ment’eva, M.V. Il’yashenko, Tech. Phys. Letters. **V. 26**, 960 (2000).

[8] A.D. Pogrebnjak, M.V. Il’yashenko, O.P. Kul’ment’eva, Yu.N. Tyurin, A.P. Kobzev, Yu.F. Ivanov, V.S. Kshnykin, Tech. Phys. **71**, 111 (2001).

[9] S.M. Duvanov and A.G. Balogh, *Nucl. Instrum. and Meth.* **B. 171**, 475 (2000).

[10] L.M. Utevsky *Diffraction Electron Microscopy in Metal Science*, Moscow, Metallurgy, 1973.

[11] A.D. Pogrebnjak, M.V. Il’yashenko, O.P. Kul’ment’eva et. al., Pis’ma v Journal Tech. Phys. **26**, 58 (2000).